Bioorganic & Medicinal Chemistry 18 (2010) 6634–6645

Contents lists available at ScienceDirect

Bioorganic & Medicinal Chemistry

journal homepage: www.elsevier.com/locate/bmc

Development of a new epidermal growth factor receptor positron emission tomography imaging agent based on the 3-cyanoquinoline core: Synthesis and biological evaluation

Federica Pisaneschi [a,c,*], Quang-De Nguyen [a], Elham Shamsaei [a], Matthias Glaser [b], Edward Robins [b], Maciej Kaliszczak [a], Graham Smith [a], Alan C. Spivey [c], Eric O. Aboagye [a,*]

[a] Comprehensive Cancer Imaging Centre, Imperial College London, Faculty of Medicine, Hammersmith Hospital Campus, Du Cane Road, London W12 0NN, United Kingdom
[b] Medical Diagnostic Discovery (part of GE Healthcare) at Hammersmith Imanet Ltd, Hammersmith Hospital, Du Cane Road, London W12 0NN, United Kingdom
[c] Department of Chemistry, Imperial College London, South Kensington Campus SW7 2AZ, United Kingdom

ARTICLE INFO

Article history:
Received 26 February 2010
Revised 22 July 2010
Accepted 2 August 2010
Available online 6 August 2010

Keywords:
EGFR
[^{18}F]-PET imaging
3-Cyanoquinoline
Click chemistry

ABSTRACT

The epidermal growth factor receptor (EGFR/c-ErbB1/HER1) is overexpressed in many cancers including breast, ovarian, endometrial, and non-small cell lung cancer. An EGFR specific imaging agent could facilitate clinical evaluation of primary tumors and/or metastases. To achieve this goal we designed and synthesized a small array of fluorine containing compounds based on a 3-cyanoquinoline core. A lead compound, **16**, incorporating 2′-fluoroethyl-1,2,3-triazole was selected for evaluation as a radioligand based on its high affinity for EGFR kinase (IC_{50} = 1.81 ± 0.18 nM), good cellular potency (IC_{50} = 21.97 ± 9.06 nM), low lipophilicity and good metabolic stability. 'Click' labeling afforded [^{18}F]**16** in 37.0 ± 3.6% decay corrected radiochemical yield based on azide [^{18}F]**14** and 7% end of synthesis (EOS) yield from aqueous fluoride. Compound [^{18}F]**16** was obtained with >99% radiochemical purity in a total synthesis time of 3 h. The compound showed good stability in vivo and a fourfold higher uptake in high EGFR expressing A431 tumor xenografts compared to low EGFR expressing HCT116 tumor xenografts. Furthermore, the radiotracer could be visualized in A431 tumor bearing mice by small animal PET imaging. Compound [^{18}F]**16** therefore constitutes a promising radiotracer for further evaluation for imaging of EGFR status.

1. Introduction

Epidermal growth factor receptor (EGFR/c-ErbB1/HER1) is overexpressed in breast, ovarian and other human cancers.[1,2] EGFR along with the other three members of the HER family (HER2, HER3 and HER4) is a transmembrane glycoprotein with an extracellular ligand-binding domain, a transmembrane domain, and an intracellular domain with tyrosine kinase activity. EGFR is activated by binding to a variety of ligands including EGF, amphiregulin and TGF-α.[3] Once activated it is believed to undergo homo- or heterodimerization followed by activation of the intrinsic protein tyrosine kinase, autophosphorylation and activation of intracellular signal transduction pathways such as phosphatidylinositol-3-kinase (PI3K)/AKT and ras/raf/MEK/MAPK.[4,3,5] Blocking EGFR activity therefore appears to be a promising strategy in the treatment of cancer. Various anti-EGFR therapies have been developed; these include monoclonal antibody inhibitors like Cetuximab (IMC-C225) which is currently in use for the treatment of colorectal and head and neck cancers and in clinical trials for metastatic breast cancer[6,7] and an arsenal of ATP competitive small molecules designed to inhibit the intracellular tyrosine kinase activity.[8] Certain compounds in this class have already been approved for clinical use (Gefitinib/Iressa,[9] Erlotinib/Tarceva[10]) whilst others are under preclinical or clinical investigation [e.g., Neratinib, pelitinib (**1**, Fig. 1)].[11,12]

Molecular imaging techniques, such as PET (Positron Emission Tomography) have the potential to provide insights into EGFR biology. Potentially, PET with EGFR probes can non-invasively determine whether the target protein is overexpressed in a specific

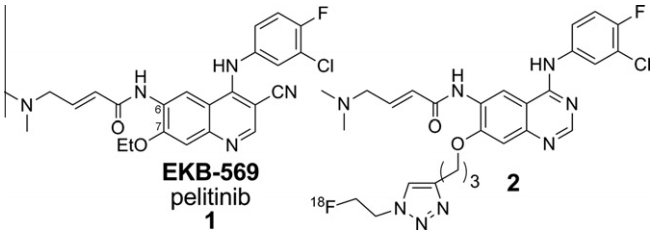

Figure 1. Structures of pelitinib (EKB-569, 1) and Neumaier's quinazoline imaging agent **2**.

* Corresponding authors.
E-mail addresses: f.pisaneschi@imperial.ac.uk (F. Pisaneschi), eric.aboagye@imperial.ac.uk (E. Aboagye).

0968-0896/$ - see front matter © 2010 Elsevier Ltd. All rights reserved.
doi:10.1016/j.bmc.2010.08.004

primary tumor or metastasis in vivo, the magnitude and duration of receptor occupancy, and target-drug interactions (including possibly the functional consequence of mutations that lead to reduced EGFR-drug interactions).

A number of previously reported therapeutics have been labeled with radionuclides, including radiometals and radiohalogens, as potential ligands for imaging EGFR.[13] Among the monoclonal antibodies, ^{64}Cu-DOTA-cetuximab showed high uptake in A431 tumors although a significant uptake in the liver was observed, partly due to the dissociation of the ^{64}Cu from the DOTA chelator.[14,15] Initial attempts to develop small molecule imaging agents focused on the introduction of radiohalogens into *reversible* EGFR inhibitors based on a 4-anilinoquinazoline core.[13,16–18] These showed promise in vitro but displayed inadequate signal to noise ratios for PET radioimaging in animal models, attributable to their relatively high lipophilicity (i.e., Log *P*) and rapid washout from cells by intracellular ATP. More recent reports by VanBrocklin et al.,[19] Mishani et al.[20–24] and Neumaier and co-workers[25] have described the evaluation of ^{11}C, ^{124}I and ^{18}F radioligands based on *irreversible* EGFR inhibitors in which an electrophilic function is incorporated at C-6 of the quinazoline core. These derivatives bind covalently to the Cys 773 located in the tyrosine kinase binding pocket of EGFR thus preventing washout by intracellular ATP and increasing potency.[26] However, despite their resistance to washout and improved in vitro inhibition profiles, radioligands of this type have thus far displayed rapid metabolic degradation[20] and/or low specific tumor uptake.[27,22] The only probe that has been evaluated in vivo by imaging in tumor bearing animals, quinazoline **2** (Fig. 1), gave non-ideal image quality, at least in part due to these features.[25]

The aim of the work described here was the synthesis and biological evaluation of ^{18}F radiolabeled irreversible imaging agents based on the known 3-cyanoquinoline irreversible inhibitor, pelitinib (EKB-569, **1**, Fig. 1).[28,29] To enable selection of the most suitable candidate radiotracer we designed a small array of fluorine containing derivatives with the intention of selecting the best candidate on the basis of high affinity to the receptor and ease of labeling. ^{18}F was chosen in preference to ^{11}C because it's long half-life time ($t_{1/2}$ = 109.8 min) allows more elaborate radiosynthesis and permits washout of non-specific binding. It was planned to introduce the ^{18}F-containing prosthetic group at the last stage of the synthesis so as to maximize the radiochemical yield of the process.

For quinazoline-based inhibitors (e.g., Neumaier's quinazoline **2**, Fig. 1), a key interaction with the EGFR binding site is the indirect hydrogen bonding of N-3 of the quinazoline core to Thr 830 mediated by a molecule of water.[29] However, molecular modeling studies indicate that in 3-cyanoquinolines (e.g., pelitinib **1**, Fig. 1), the 3-cyano group hydrogen bonds directly to Thr 830 without the involvement of a water molecule.[29] We speculated that this latter, probably more entropically favored, interaction might be exploited in a derived imaging agent to allow for higher uptake into the tumor and result in more specific imaging signal. In line with the design criteria applied previously to irreversible quinazoline-based tracer candidates, we wanted to retain an aniline moiety at C-4 to optimally occupy the active site hydrophilic pocket and a Michael acceptor (incorporating a tethered amine) at C-6 to covalently bind to Cys 773.[29] Consequently, it was decided that compound **1** would be modified by the addition of fluorine containing groups at the terminus of the C-6 Michael acceptor (with minimal structural perturbation) or at the C-7 position (which points outside the active site and does not appear to play an important role in binding). In the interest of maximizing resistance to metabolic degradation we were also interested in exploring the reportedly increased stability of Michael acceptors modified with secondary rather than tertiary amines.[30]

2. Results

2.1. Chemistry

Pelitinib (EKB-569, **1**) was synthesized by the procedure of Wissner et al.[29,31] via the key 3-cyanoquinoline intermediate **3**. This latter compound also provided the starting point for the synthesis of three potential labeling precursors **6**, **8**, and **10**, which incorporate modified C-6 Michael acceptor units. Compound **6** incorporates a methylamine unit in place of the dimethylamine unit found in pelitinib (**1**) so as to allow label introduction via alkylation or reductive amination. This derivative was prepared by $AlMe_3$ mediated amidation with methyl (*E*)-4-(*tert*-butoxycarbonylmethylamino)-but-2-enoate **4** (47%)[32] followed by Boc removal using 10% concd HCl in dioxane (78%). Compound **8** incorporates a Boc-propargylamine unit in place of the dimethylamine unit found in pelitinib (**1**) so as to allow label introduction via copper(I) catalyzed Huisgen 1,3-dipolar cycloaddition (the 'click' reaction).[33–36] This derivative was prepared by $AlMe_3$ mediated amidation with ethyl (*E*)-4-(*tert*-butoxycarbonyl-prop-2-ynyl-amino)-but-2-enoate **7** (see Section 4, 68%). Compound **10** incorporates a terminal alkyne in place of the dimethylaminomethyl unit found in pelitinib (**1**) so as to allow an alternative mode of label introduction via 'click' cycloaddition. This derivative was prepared by $AlMe_3$ mediated amidation with methyl (*E*)-pent-2-en-4-ynoate **9** (20%)[37] (Scheme 1).

Derivatization of *N*-methyl amine **6** in a manner amenable to the introduction of an ^{18}F radiolabel was explored by alkylation and via reductive amination. Alkylation of amine **6** with 1-fluoro-2-mesyloxy ethane (**11**) in CH_2Cl_2 gave the *N*-fluoroethyl product **12** in 33% yield following difficult chromatographic separation from unidentified by-products. Alternatively, reductive amination of 4-fluoro benzaldehyde by quinoline **6** was achieved using $NaBH(OAc)_3$ and gave the 4-fluorobenzyl product **13** in 21% yield following rapid chromatography (Scheme 2).

Derivatization of *N*-Boc-propargylamine **8** and enyne containing quinoline **10** in a manner amenable to the introduction of an ^{18}F radiolabel was envisaged via 'click' cycloaddition with a fluorine containing azide partner. Propargylamine **8** was therefore reacted with 1-fluoro-2-ethyl azide (**14**)[38] under Cu(I) catalysis and microwave irradiation[39] to give fluorotriazole-containing quinoline **16** as

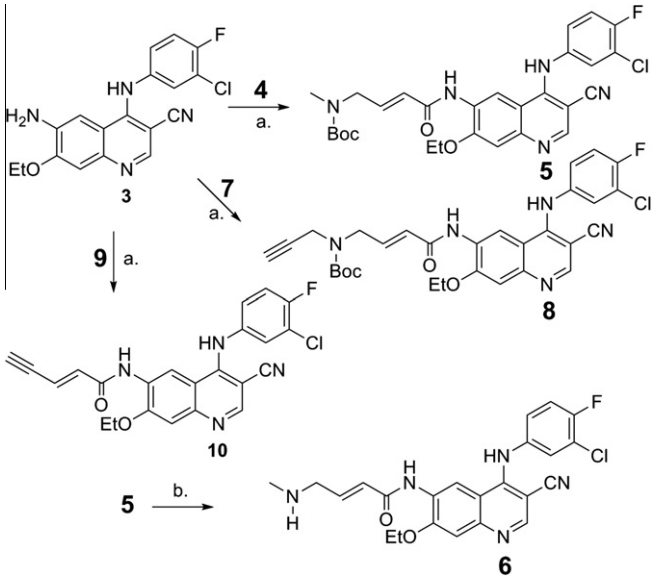

Scheme 1. Reagents and conditions: (a) $AlMe_3$, CH_2Cl_2, rt, (**5**: 47%, **8**: 68%, **10**: 20%). (b) (i) dioxane/HCl, 10:1, rt, 30 min; (ii) K_2CO_3, H_2O, 14 h (78%).

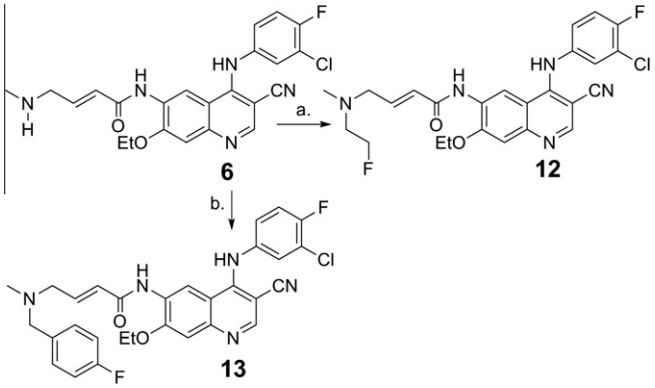

Scheme 2. Reagents and conditions: (a) **11**, Et_3N, CH_2Cl_2, 18 h at rt and 24 h at reflux (33%). (b) *p*-fluorobenzaldehyde, AcOH, $NaBH(OAc)_3$, 1,2-dichloroethane, 14 h (21%).

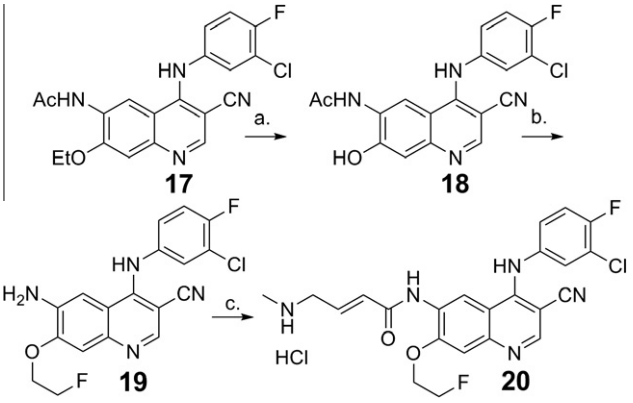

Scheme 4. Reagents and conditions: (a) BBr_3, CH_2Cl_2, rt (40%); (b) (i) **11**, K_2CO_3, DMF, 70 °C, 18 h (83%); (ii) concd HCl, H_2O, 120 °C, 1.5 h (53%); (c) (i) **4**, $AlMe_3$, toluene, rt, 14 h (61%); (ii) concd HCl, dioxane, rt (67%).

an HCl salt following Boc removal using HCl in 1,4-dioxane. Similarly, enyne **10** reacted with azide **14** to give fluorotriazole-containing quinoline **15** in 32% yield. In both cases, the final yields were compromised by the apparent instability of the Michael acceptor precursors under the reaction conditions (Scheme 3).

Quinoline **20** was designed as a direct analogue of quinoline **6** but containing a 2-fluoroethoxy group in place of the C-7 ethoxy group. The synthesis route started from quinoline **17**,[29,31] which is an intermediate in the Wissner synthesis of pelitinib (EKB-569, **1**), and was not designed for direct translation into a labeling method but rather as the most convenient entry for SAR purposes. The C-7 ethyl ether in quinoline **17** was removed by treatment with BBr_3 and the resulting quinoline **18** was alkylated with 1-fluoro-2-mesyloxy ethane (**11**) under basic conditions followed by acetamide hydrolysis to give 7-(2-fluoroethoxy)quinoline **19**. $AlMe_3$ mediated amidation with methyl (*E*)-4-(*tert*-butoxycarbonyl-methyl-amino)-but-2-enoate **4** and Boc removal by treatment with HCl in 1,4-dioxane gave the target quinoline **20** as its HCl salt (Scheme 4).

None of the aforementioned 'cold' procedures were optimized as this was not required in order to prepare sufficient material for subsequent evaluation (see below).

2.2. Radiochemistry

Alkyne containing quinoline **21** was obtained from compound **8** by treatment with concd HCl in 1,4-dioxane in quantitative yield. Compound **21** was labeled by cycloaddition under Cu(I) catalysis by using 2-[^{18}F]fluoroethylazide [^{18}F]**14** following a published procedure (Scheme 5).

2-[^{18}F]Fluoroethylazide [^{18}F]**14** was synthesized from the corresponding tosyloxyethylazide **22** and [^{18}F]KF/Kryptofix 222 at 80 °C for 15 min. The product was purified and collected by distillation in MeCN; it was obtained with a 43.0 ± 4.1% (n = 12) decay corrected radiochemical yield. Precursor **21** was dissolved in MeCN/water, 1:1, mixed with the catalytic system and then reacted with the azide [^{18}F]**14** at 80 °C for 15 min. The crude compound [^{18}F]**16** was purified by semipreparative HPLC in a 37.0 ± 3.6% (n = 12) decay corrected radiochemical yield from azide [^{18}F]**14** (EOS = 7% from aqueous [^{18}F]fluoride) and >99% radiochemical purity. Compound [^{18}F]**16** was formulated by solid-phase extraction with an efficiency of ~90%. The identity of [^{18}F]**16** was confirmed by co-elution with the non-radioactive compound. The formulated compound was obtained with a specific activity (SA) of 48–685 GBq/μmol at EOS. The radioimaging agent [^{18}F]**16** was stable for at least 4 h after formulation in phosphate buffered saline (PBS). The radiosynthesis including formulation took 3 h in total.

2.3. Biology

A key design goal is the introduction of radiolabeled motifs without significant detriment to EGFR inhibitory affinity (asurrogate for binding) relative to the starting quinoline **1**. Therefore, assessment of the EGFR tyrosine kinase activity of control quinolines **1** together with quinolines **6**, **12**, **13**, **15**, **16**, **20**, and **21** was

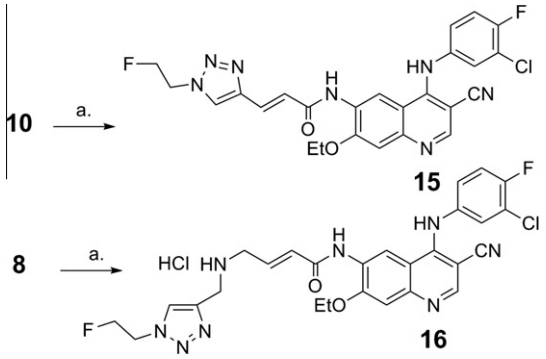

Scheme 3. Reagents and conditions: (a) **14**, Cu powder, $CuSO_4$, water, MW 125 °C, 15 min (**15**: 32%, **16**: 19%); (b) dioxane/HCl, 10:1, 1 h (99%).

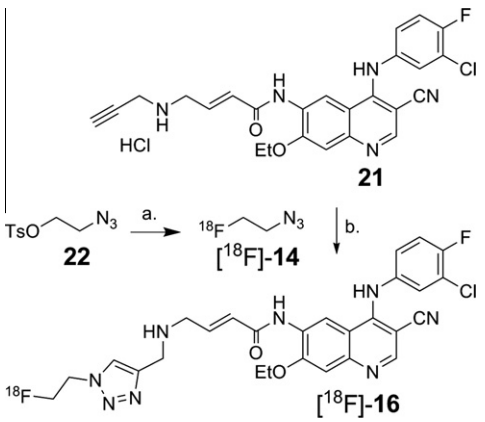

Scheme 5. Reagents and conditions: (a) [^{18}F]KF/Kryptofix 222, 80 °C, 15 min (43%); (b) $CuSO_4$, Na ascorbate, pH 6, MeCN, H_2O (37%).

carried out using a cell-free kinase activity inhibition assay as detailed in Section 4. 4-[(3-Bromophenyl)amino]-6,7-diaminoquinazoline (BPDQ),[40] a quinazoline-based EGFR inhibitor, was also included in this assay as a further reference standard. Concentrations of the compounds that inhibited EGFR kinase activity by 50% (IC_{50}) were calculated and are reported in Table 1.

All eight compounds inhibited EGFR kinase activity with IC_{50} values in the low- or sub-nanomolar range which compares well with that of BPDQ (Table 1). Compound **1** appeared more potent than previously reported by Wissner et al.[29] presumably because of differences in the assay used. The same authors have shown that compound **1** functions as an irreversible inhibitor of EGFR. The IC_{50} values are probably best interpreted in the context of reversible inhibition, as well as irreversible covalent binding resulting from interactions with the Michael acceptor (and other reactive) moieties. The sub-nanomolar kinase activity observed with compounds **1** and **6** was retained in compounds **12** and **13** demonstrating tolerance for small and large fluorine containing substituents on the tertiary amine group. Fluorine substitution at the C-7 position was also tolerated as reflected in the comparably low IC_{50} valued measured for compounds **6** and **20**. Of interest to the application of 'click' radiochemistry, incorporation of a fluoroethyl triazole onto the Michael acceptor—exemplified by quinolines **15** and **16**—was tolerated, with quinoline **16** being twofold more active than **15**. The activity of triazole derivatives **15** and **16** was reduced 10–20-fold relative to quinoline **1**; the reason for this is unclear since previous modeling studies place the amine substituents at the edge of the kinase pocket. In addition, a bulky substituent was tolerated in the case of quinoline **13**. Surprisingly, the activity of the alkyne-containing quinoline **21** was in the picomolar range (30 pM) possibly due to a previously undocumented π–π interaction that may also help to explain the high affinity of fluorobenzyl quinoline **13**.

Given the encouraging inhibitory EGFR kinase activity of the compound series in the cell-free system, we examined cellular activity—the ability of the compounds to be transported across cell membranes and to inhibit EGFR autophosphorylation—in highly EGFR expressing A431 cells.[41] Following a protocol previously reported by Rabindran et al.,[11] we measured the potency of the compounds to inhibit autophosphorylation of EGFR after 3 h of drug incubation and a further 2 h of washing with drug free medium. Due to the washing steps, the protocol permits the effect of irreversible binding activity to be quantified. Typical immunoblots demonstrating inhibition of EGFR autophosphorylation are shown in Figure 2. In these studies the drug did not inhibit the expression of total EGFR protein. The inhibitory activity of compounds **1**, **6**, **12**, **13**, **16**, **20**, and **21** on cellular EGFR autophosphorylation, (Table 1) translated well from that assessed in the cell-free system, with IC_{50} values in the low nanomolar range. Interestingly, no cellular activity was apparent when dosing with quinoline **15**. Furthermore, the cellular activity of quinoline **21** was in the low nanomolar range indicating that, although potent, the high affinity of this alkyne in the kinase assay did not directly translate into cellular activity.

As a consequence of the in vitro screening, quinoline **16** was selected for further development because of its high binding affinity, structural novelty, and the ease of click radiolabeling. The in vivo

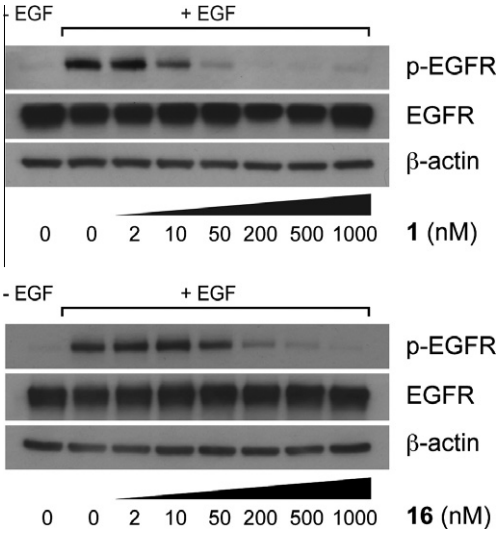

Figure 2. Cellular activity of quinolines **1** and **16** assessed by Western blots analysis of phosphorylated EGFR (p-EGFR) and total EGFR (EGFR).

Table 1
EGFR kinase activity inhibition profile for quinolines **1**, **6**, **12**, **13**, **15**, **16**, **20** and **21**

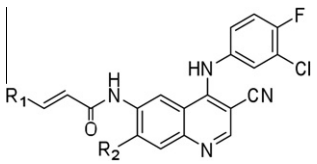

	R_1	R_2	IC_{50} (nM)		
			EGFR kinase activity	A431 EGFR autophosphorylation[a]	*c* log *P*[b]
BPDQ			0.81 ± 0.01	>1000	2.57
1	CH_2NMe_2	OEt	0.24 ± 0.02	8.02 ± 0.75	4.18
6	CH_2NHMe	OEt	0.25 ± 0.06	5.35 ± 1.52	3.80
12	$CH_2NH(Me)CH_2CH_2F$	OEt	0.80 ± 0.04	23.02 ± 12.00	4.38
13	$CH_2N(Me)$(4-fluorobenzyl)	OEt	0.57 ± 0.12	16.52 ± 8.38	6.05
15	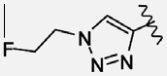	OEt	4.05 ± 0.57	>1000	4.45
16	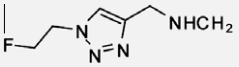	OEt	1.81 ± 0.18	21.97 ± 9.06	3.85
20	CH_2NHMe	OCH_2CH_2F	0.29 ± 0.03	8.12 ± 2.03	3.64
21	$CH{\equiv}CCH_2NHCH_2$	OEt	0.03 ± 0.01	60.20 ± 17.10	3.94

[a] Data were extracted from the concentration versus p-EGFR/total EGFR Western blot absorbance ratio. Data are mean ± sem, $n = 3$ replicates.
[b] *c* log *P* are calculated by ChemAxon's MarvinSketch, version 5.2.6.

evaluation of the imaging agent [^{18}F]**16** focused on the assessment of its metabolic stability and its ability to be taken up into a EGFR expressing xenograft, A431, in animals. Non-specific binding plagued development of earlier generation radiotracers (quinazolines) for imaging EGFR.[22] We initially assessed two of the likely reasons for non-specific binding—poor metabolic stability and poor pharmacokinetics—in the context of [^{18}F]**16** to inform the development of this and the next generation of EGFR imaging agents. We investigated the in vivo metabolic stability of [^{18}F]**16** in non-tumor bearing mice by analyzing liver and plasma extracts at 2, 30, and 60 min post injection. Sample analysis was accomplished by radio-HPLC. Typical radiochromatograms are shown in Figure 3 and the results are summarized in Table 2. At 2 min, only parent compound was observed in liver and plasma. A low level more polar peak was seen in liver at 30 and 60 min and a similar radioactive metabolite was seen in plasma. This metabolic stability data demonstrates that the parent radiotracer [^{18}F]**16** remains a major component of both liver and plasma even at 60 min post injection; indicative of relatively good stability in vivo.

The 60 min tissue biodistribution A431 tumor bearing mice, expressed as tissue to blood ratios, has been measured and the results are shown in Figure 4. Tumor (A431 xenograft) uptake was approximately fourfold higher than that of muscle (%ID/g in tumor = 0.082 ± 0.022 and %ID/g in muscle = 0.018 ± 0.004, see Supplementary data, Table S1). Low radioactivity was also observed in other organs including bone, brain, and heart. The low uptake in bone suggests that the radiotracer does not undergo defluorination. The radiotracer appeared to be eliminated via both the hepatobiliary and renal routes, as the highest tissue radioactivities were found in the gallbladder and the urine. Elimination of the radiotracer into the gut may also account for the high radioactivity in the early part of the intestine (Fig. 4).

We further assessed the potency of compound [^{18}F]**16** to detect high EGFR expressing A431 xenografts relative to low EGFR expressing HCT116 xenografts by small animal PET imaging. PET images from representative A431 and HCT116 tumor bearing mice with [^{18}F]**16** (Fig. 5) demonstrated localization and visualization of the tumor, particularly in A431. The time activity curves (TACs) of A431 and HCT116 tumors extracted from the PET data (Fig. 5) showed more rapid washout of the radiotracer from HCT116 tumors. Significant radiotracer localization was also seen in the abdominal region consistent with the biodistribution data. The PET data were corroborated by ex vivo tumor uptake and western blot analysis of EGFR protein content of the two tumor types

Table 2
In vivo metabolism of compound [^{18}F]**16** (SA = 685 GBq/μmol) at selected time points, showing the proportion of compound [^{18}F]**16** present in plasma and liver extracts[a]

Time (min)	Parent (liver)	Parent (plasma)
2	95.00 ± 1.00	98.92 ± 1.06
30	85.06 ± 1.75	62.81 ± 1.70
60	75.45 ± 2.73	49.75 ± 6.27

[a] The extracts were analyzed by radio-HPLC [50% MeCN (0.085% H_3PO_4)]. The values are the average of three independent studies per time point. Proportion of compound [^{18}F]**16** in plasma and liver were calculated by comparison of compound [^{18}F]**16** peak to total radioactivity present on chromatogram. The efficiency of the extraction from plasma was 83.5%.

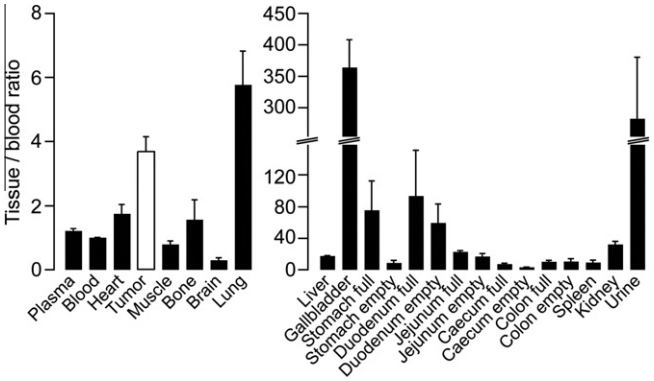

Figure 4. Tissue distribution of compound [^{18}F]**16** in untreated tumor bearing mice at 60 min (sacrifice time point). Data are ±SEM; n = 3 mice.

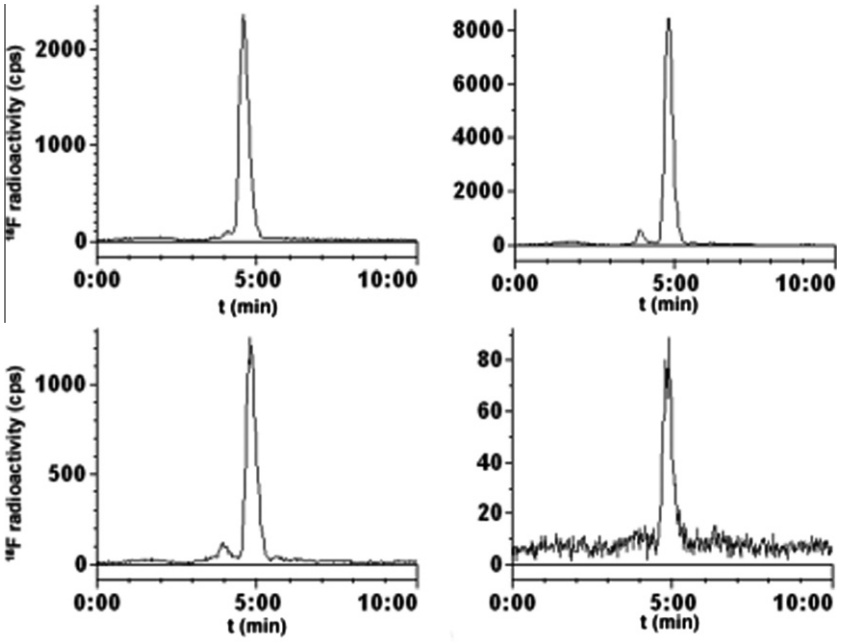

Figure 3. In vivo metabolism of compound [^{18}F]**16** in mice liver as assessed by radio-HPLC. Top panel: reference compound and 2 min, respectively. Bottom panel: 30 min and 60 min, respectively.

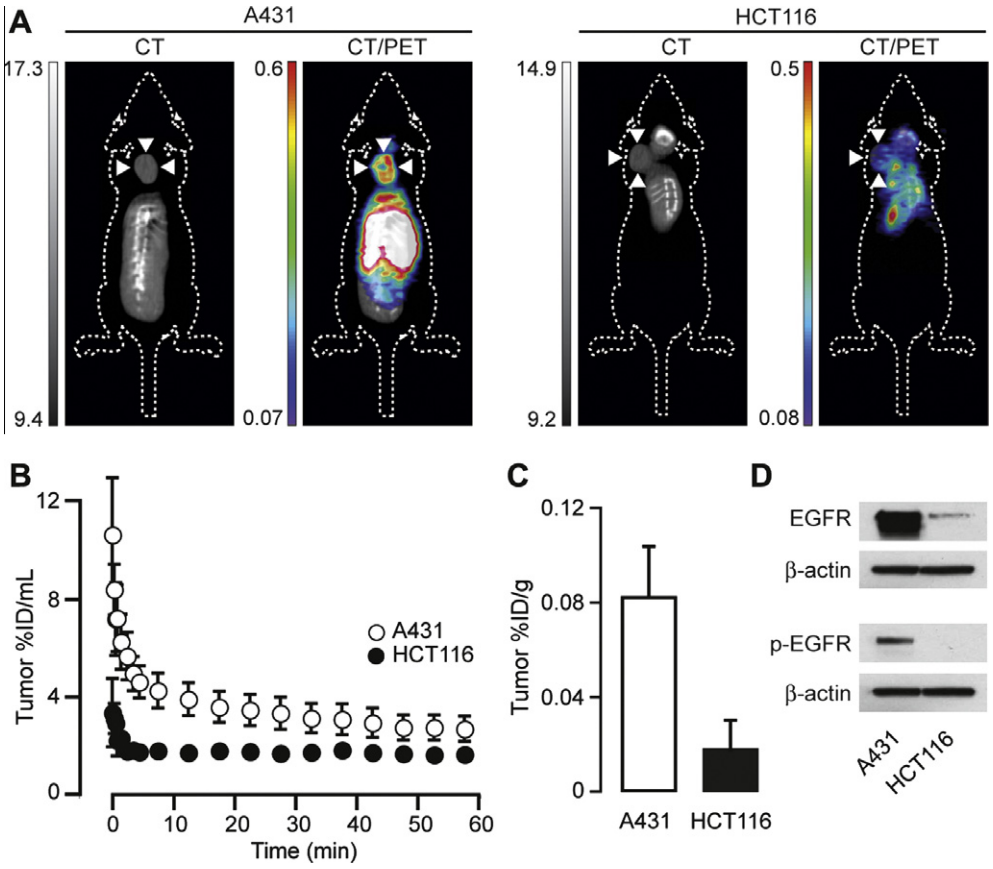

Figure 5. Computed tomography and compound [^{18}F]**16** PET images (summed dynamic) of representative A431 and HCT116 xenograft-bearing mice (SA = 48 GBq/μmol), together with time versus radioactivity curves and tumor uptake measured by γ-counting. White arrowheads on the PET images indicate the tumor seen on the computed tomography images. Western blots of the two cell lines are also shown for EGFR and phosphorylated EGFR–p-EGFR; β-actin was used as loading control.

(Fig. 5). There was a fourfold higher uptake in A431 xenografts compared to HCT116 xenografts.

3. Discussion and conclusion

Previous PET imaging studies with irreversible inhibitors of EGFR have suggested that selectivity and metabolic stability are likely to be key attributes of radiotracers if they are to display good uptake by tumors and give good image quality.[13] With this in mind, we selected the 3-cyanoquinoline therapeutic agent pelitinib (**1**), first reported by Tsou et al.,[29,31,43] as a template on which to introduce an ^{18}F label. The 3-cyanoquinoline core, as indicated in the introduction, was chosen in preference to the quinazoline core because it was hoped that it might engender higher uptake into the tumor and result in more specific imaging signal. The C-4 aniline and C-6 aminocrotonylamide moieties were retained to ensure selectivity for EGFR and irreversible binding to the active site Cys 773 via Michael addition, respectively.[29] A small array of ^{19}F containing 3-cyanoquinolines was therefore synthesized (compounds **12**, **13**, **15**, **16**, and **20**) and these compounds were tested for their ability to inhibit the intracellular tyrosine kinase autophosphorylation activity of EGFR. The fluorine containing groups were introduced onto both the Michael acceptor moiety and the C-7 ether position of the quinoline core. Previous studies[29,31] have indicated some tolerance for substitution at these sites, which made the C-6 and C-7 positions attractive for modification in the present investigation. The synthetic routes developed to prepare the C-6 derivatives were designed such that they would be amenable to preparation of the corresponding [^{18}F]-fluorine containing congeners from readily available radiolabeled prosthetic groups (i.e., [^{18}F]-1-fluoro-2-ethyltosylate,[44] [^{18}F]-*p*-fluorobenzaldehyde[45] or [^{18}F]-1-fluoro-2-ethylazide[46]). The route for preparation of the C-7 modified 2-fluoroethyl ether (quinoline **20**) did not share this anticipated ease of translation into a convenient late-stage labeling method but gave expedient access to the ^{19}F product in order to evaluate its properties. The eight compounds were screened for their EGFR tyrosine kinase activity inhibition using BPDQ as positive control. The non-fluorinated quinolines **1**, **6**, and **21** were also screened; compound **1** was used as a standard and compounds **6** and **21** were the potential radiochemical precursors for those fluorinated quinolines most likely to be translated into imaging agents. We assessed these latter compounds in order to better understand the potential impact of residual impurities in an eventual radiopharmaceutical formulation.

As expected, in the cell-free kinase activity inhibition assay, the sub-nanomolar binding affinity showed by quinolines **1** and **6** was retained in quinolines **12** and **13** despite the increased bulk of the tertiary amine substituents. Surprisingly, the activity of the alkyne-containing quinoline **21** was in the picomolar range, possibly because of secondary interactions of the alkyne group with the binding site of the enzyme, a feature unfortunately not retained in compound **16**. Nevertheless, the low nanomolar affinity of compound **16** was considered sufficient to allow further in vivo characterization of EGFR related activities. The slightly higher IC_{50} of compound **15** may be attributable to the replacement of the tertiary amine, which acts as internal base, with the significantly less basic triazole ring (vide infra). Finally, quinoline **20**, designed to be a direct analogue of quinoline **6**, but containing a 2-fluoroethoxy

group in place of the C-7 ethoxy group, showed the same activity as compound **6** confirming that the C-7 group is not involved in the binding with the EGFR tyrosine kinase enzyme. With these preliminary encouraging results in hand, the candidate compounds were screened for their ability to inhibit autophosphorylation in the human epithelial carcinoma A431 cell line. All the compounds were active at nanomolar concentrations except for compound **15** and the positive control BPDQ. Compounds **12**, **13**, **16**, and **21** were, however, 10-fold less active than reference compounds **1** and **6**.

The lack of activity of compound **15** might be accounted for by its inability to cross the cell membrane, although its physicochemical properties are comparable with the other members of the series. Alternatively, the lack of activity of compound **15** in cells might be a consequence of it having a more reversible interaction with the kinase, as the methodology we employed for measuring cellular activity (with washing steps) permits mainly irreversible inhibition to be quantified. This would be consistent with the lack of activity of BPDQ which is known to be a reversible inhibitor of EGFR.[40] A reversible interaction of compound **15** with EGFR kinase is possible since replacement of the amine group at the terminus of the Michael acceptor with a nitrogen atom contained within a triazole ring system may prevent the Michael reaction of the Cys 773 thiol from occurring; this would result in loss of activity in the cellular assay. The low basicity of the triazole nitrogen and/or the lack of conformational flexibility of this group could well be preventing the Michael acceptor from reacting efficiently. In particular, the aromatic nature of the triazole ring combined with the sp^2 hybridisation state of the N-3 atom ensures that its basicity is likely $\sim 10^9$-fold lower than that of the secondary/tertiary amines. Moreover, the triazole ring has an extended planar π-electron system conjugated to the amide carbonyl group and consequently will have a significant barrier to rotation to give the correct orientation in which this nitrogen lone pair can assist with general base catalysis of the attack of the Cys 773 thiol at the γ position of the enamide unit.

We interpret the lower activity of compounds **12**, **13**, **16**, and **21** relative to compounds **1** and **6** as suggesting that bulkier groups on the amine of the Michael acceptor have a negative effect on the cellular activity. This effect is particularly apparent for compound **21** whose activity decreases 2000-fold in the cell relative to its activity in the cell-free assay. This may be due to side reactions of the alkyne moiety with the cell surface which could partially prevent its penetration into the cell, although no specific evidence for this was obtained. Compound **20**, where the Michael acceptor has not been modified, showed comparable activity to compounds **1** and **6**.

Quinoline **16** was then selected for further development as a first generation 3-cyanoquinoline imaging agent. This compound balanced high binding affinity in vitro, structural novelty, and a radiosynthesis method via efficient 'click' chemistry. Cognizant of the importance of a favorable metabolic profile, we decided to test compound **16** for its stability in mouse and human liver microsomes in comparison with compound **6**. Interestingly, after 60 min of incubation, only the parent compound was detected by HPLC (data not shown). The absence of metabolites is consistent with the notion that secondary amine substituted Michael acceptors display relatively high metabolic stability (cf. tertiary amine analogues).[30] The C-7 ethoxy group also appears to be relatively stable in this regard. The metabolic stability of the radiolabeled compound [^{18}F]**16** was then explored further in vivo; metabolism studies were carried out by radio-HPLC analysis of liver and plasma samples of non-tumor bearing mice treated with [^{18}F]**16** at three time points (2, 30, and 60 min). Tracer [^{18}F]**16** appeared to be stable in the liver as the parent compound was by far the major component present after 60 min. In plasma, this was the case after 2 min, but a metabolite appeared after 30 min and increased after 60 min. The tissue distribution of tracer [^{18}F]**16** at 60 min post injection showed that the radiotracer is probably eliminated via both the hepatobiliary and renal routes. Elimination of the radiotracer into the gut may also account for the high radioactivity in the early part of the intestine. Compared to other radiotracers reported in the literature,[22] tracer [^{18}F]**16** shows reduced kidney, liver and lung uptake which may be related to its relatively high metabolic stability and also suggests that tracer [^{18}F]**16** may be a more suitable candidate for upper torso imaging. The tumor uptake in A431 xenografts compares favorably with data reported in the literature for tracers with a quinazoline core.[22] The low uptake in bone suggests that the radiotracer does not undergo defluorination. We also assessed the potency of compound [^{18}F]**16** to detect A431 and HCT116 xenografts by small animal PET imaging. Although high non-specific localization was seen in the elimination organs, the uptake into the tumor was clearly visible, particularly for A431. Specificity of radiotracer uptake was demonstrated by the higher uptake of the radiotracer in high EGFR expressing A431 tumor xenografts compared to low EGFR expressing HCT116 tumor xenografts. The high level of radioactivity in the intestine is of particular concern as this would preclude use of this tracer for imaging, for example, colorectal cancer but should not limit its application for other EGFR overexpressing cancers, for example, breast cancer.

In conclusion, compound [^{18}F]**16** represents a first generation, 3-cyanoquoline-based selective EGFR radioimaging agent. The 3-cyanoquinoline core and C-6 Michael acceptor bearing a triazole functionalized secondary amine terminus appear to confer greater metabolic stability than has been previously reported for related EGFR probes. The biodistribution profile in normal tissues, the selectivity of radiotracer uptake in A431 versus HCT116 and the ability to detect A431 tumors in animal models by PET imaging certainly encourage further investigations into the use of this reagent for EGFR imaging. The initial results reported herein suggest that modifications of the structure of compound [^{18}F]**16** designed to modulate the pharmacokinetic properties will be necessary to further improve uptake into the tumor and reduce non-specific binding. Further studies are currently ongoing in our laboratories.

4. Experimental section

4.1. Chemistry and radiochemistry

Solvents were distilled as follows: THF and Et_2O over Na-benzophenone ketyl, toluene over Na, and CH_2Cl_2 over CaH_2. Reagents were used as commercially supplied unless otherwise stated and handled in accordance with COSHH regulations. Flash chromatography (FC) was carried out on Silica gel (BDH Silica Gel for FC). NMR spectra were recorded at 400 MHz on a Bruker AV-400 or Bruker DX-400 instrument or at 500 MHz on a Brucker AV-500 instrument. Chemical shifts (δ) are given in parts per million (ppm) as referenced to the appropriate residual solvent peak. The reference for ^{19}F NMR is $CFCl_3$ (= 0 ppm). Broad signals are assigned as br. ^{13}C chemical shifts (δ) are assigned as s, d, t, and q, for C, CH, CH_2, and CH_3, respectively. Coupling constants (J) are given in Hz. Infrared spectra were recorded as thin films, on Perkin–Elmer Paragon 1000 Fourier transform spectrometer or as solids, on Pelkin–Elmer Spectrum 100 Fourier transform spectrometer. Only selected absorbances (ν_{max}) are reported. Low resolution and high-resolution mass spectra were recorded on a VG Prospec spectrometer, with molecular ions and major peaks being reported. Intensities are given as percentages of the base peak. HR-MS values are valid to ±5 ppm. Melting points of solid compounds were higher than 250 °C and decomposition was observed. [^{18}F]Fluoride was produced by a cyclotron (PET trace) using the ^{18}O(p,n)^{18}F nuclear reaction with 16.4 MeV proton irradiation of an enriched [^{18}O]H_2O target.

4.2. HPLC methods

(a) Preparative radio-HPLC was carried out on a Beckman System Gold equipped with a Bioscan Flowcount FC-3400 PIN diode detector (Lablogic) and a linear UV-200 detector (wavelength 254 nm). A Phenomenex Luna C18 150 mm × 10 mm HPLC column and a isocratic mobile phase of water and 20% acetonitrile (0.085% H_3PO_4) and flow rate 3 mL/min. (b) Analytical radio-HPLC was carried out as above but using a Bioscan Flowcount FC3200 sodium iodide/PMT gamma detector (Lablogic), a Thermo Spectra SERIES UV150 (wavelength 254 nm), and a Phenomenex Luna 50 mm × 4.6 mm (3 μm) column with an isocratic mobile phase of water and 22% acetonitrile (0.1% TFA), flow rate 1 mL/min.

4.3. Synthesis

Compounds **1**,[29] **3**,[29] **4**,[32] and **9**[37] were synthesized according to established literature procedures and ^{1}H NMR spectral data were consistent with those previously reported.

4.3.1. (*E*)-4-(*tert*-Butoxycarbonyl-prop-2-ynylamino)-but-2-enoic acid methyl ester (7)

4-Bromo methylcrotonate (1 g, 5.6 mmol) was dissolved in dry THF (10 mL) and propargyl amine (961 μL, 14 mmol) was added dropwise at −20 °C. The resulting mixture was stirred at −20 °C for 4 h then cooled to −65 °C. Boc_2O (4.9 g, 22.3 mmol) and Et_3N (4 mL, 27.9 mmol) were then added in turn and the mixture stirred at −65 °C → rt for 14 h. The white solid was filtered off and the mother liqueur was concentrated under reduced pressure, dissolved in CH_2Cl_2 (30 mL) and washed with water (20 mL), HCl 1 M (20 mL), water (20 mL), and brine (20 mL) and finally dried over $MgSO_4$. The crude residue was purified by FC (Et_2O/petroleum ether, 1:4; R_f = 0.12) to give the title compound (681 mg, 49%) as colorless oil.

^{1}H NMR (400 MHz, $CDCl_3$) δ 6.90 (dt, J = 15.7, 5.3, 1H), 5.93 (d, J = 15.7, 1H), 4.19–3.91 (m, 4H), 3.77 (s, 3H), 2.24 (t, J = 2.4, 1H), 1.49 (s, 9H); ^{13}C NMR (101 MHz, $CDCl_3$) δ 166.5 (s), 154.6 (s), 143.6 (d), 122.1 and 121.8 (d), 81.0 (s), 78.9 (d), 72.3 (s), 71.9 (s), 51.7 (q), 47.0 and 46.8 (t), 36.4 and 35.9 (t), 28.3 (q, 3C); IR: ν_{max} 3263, 2976, 2361, 1699, 1450, 1273, 1167 cm^{-1}; MS (ESI): m/z (%) 276 [MNa^+] (35); HR-MS (ESI) calcd for $C_{13}H_{19}NO_4Na$: 276.1211, found 276.1212 (Δ −0.4 ppm).

4.3.2. General procedure for the synthesis of compounds 5, 8, 10, and Boc-20

The amino quinolines **3** or **19** (1 equiv) and the Michael acceptor **4**, **7** or **9** (1.5 equiv) were suspended and sonicated in dry CH_2Cl_2 (0.06 M) and $AlMe_3$ (2.0 M solution in hexane, 2 equiv) was added dropwise at rt. The mixture was stirred at rt and monitored by TLC until the starting quinoline had disappeared. The mixture was quenched with a saturated solution of $NaHCO_3$ and the phases were separated. The aqueous layer was extracted twice with equal volumes of CH_2Cl_2 and the combined organic layers washed with equal volume of brine and dried over $MgSO_4$. The crude mixture was purified by FC or plate silica gel TLC.

4.3.2.1. {(E)-3-[4-(3-Chloro-4-fluorophenylamino)-3-cyano-7-ethoxyquinolin-6-ylcarbamoyl]-allyl}-methylcarbamic acid tert-butyl ester (5). Yellow semisolid, 47% yield; R_f = 0.12 (petroleum ether/AcOEt, 1:2); ^{1}H NMR (400 MHz, $CDCl_3$): δ 9.20 (s, 1H), 8.53 (s, 1H), 8.07 (s, 1H), 7.91 (br s, 1H), 7.31–7.21 (m, 1H), 7.21–7.13 (m, 1H), 7.12–6.88 (m, 3H), 6.15–6.02 (m, 1H), 4.38–4.27 (m, 2H), 4.08 (br s, 2H), 2.98–2.85 (m, 3H), 1.61 (t, J = 6.9 Hz, 3H), 1.53 (s, 9H); ^{13}C NMR (101 MHz, $CDCl_3$): δ 164.4 (s), 156.6 [s (d, J_{CF} = 247.8)], 155.6 (s), 152.0 (d), 150.8 (s), 149.4 (s), 147.2 (s), 143.3 and 142.3 (d), 135.7 (s), 127.3 (s), 125.8 (d), 124.3 (d), 123.1 (d), 121.1 [s (d, J_{CF} = 18.9)], 116.8 (s), 116.4 [d (d, J_{CF} = 22.3)], 113.1 (s), 109.9 and 109.5 (d), 108.4 (d), 88.3 (s), 79.9 (s), 65.0 (t), 49.9 and 49.3 (t), 34.3 (q), 28.2 (q, 3C), 14.4 (q); IR: ν_{max} 3347, 2928, 2211, 1681, 1535, 1498, 1391, 1145 (MS (ESI): m/z (%) 554 [MH^+] (100); HR-MS (ESI) calcd for $C_{28}H_{30}ClFN_5O_4$: 554.1970, found 554.1981 (Δ 2.0 ppm).

4.3.2.2. {(E)-3-[4-(3-Chloro-4-fluorophenylamino)-3-cyano-7-ethoxyquinolin-6-ylcarbamoyl]-allyl}-prop-2-ynyl carbamic acid tert-butyl ester (8). Colorless oil; 68% yield, R_f = 0.14 (eluent: AcOEt/Et_2O, 10:1); ^{1}H NMR (400 MHz, $CDCl_3$) δ 9.18 (s, 1H), 8.39 (s, 1H), 8.17 (br s, 1H), 7.96 (s, 1H), 7.08 (s, 1H), 7.05–6.94 (m, 2H), 6.89 (t, J = 8.6, 1H), 6.68 (m, 1H), 6.08 (d, J = 14.9, 1H), 4.22 (q, J = 6.9, 2H), 4.13 (d, J = 4.2, 2H), 4.05 and 3.90 (br s, 2H), 2.25 (t, J = 2.2, 1H), 1.58 (t, J = 7.0, 3H), 1.48 (s, 9H); ^{13}C NMR (101 MHz, $CDCl_3$) δ 164.3 (s), 155.8 [s (d, J_{CF} = 249.8 Hz], 154.7 (s), 152.1 (d), 151.0 (s), 149.6 (s), 147.3 (s), 142.7 and 142.2 (d), 135.7 (s), 127.5 (s), 126.1 (d), 125.5 (d), 123.43 and 123.36 (d), 121.2 [s (d, J_{CF} = 18.9)], 116.8 (s), 116.5 [d (d, J_{CF} = 22.3)], 113.2 (s), 109.7 (d), 108.5 (d), 88.5 (d), 81.0 (s), 79.1 (s), 72.2 and 71.9 (d), 65.1 (t), 47.0 (t), 36.5 and 35.9 (t), 28.3 (q; 3C), 14.1 (q); IR: ν_{max} 3412, 3307, 2980, 2930, 2252, 2214, 1690, 1682, 1537, 1250, 734 cm^{-1}; MS (ESI): m/z (%) 578 [MH^+] (100); HR-MS (ESI) calcd for $C_{30}H_{30}N_5O_4FCl$: 578.1970, found 578.1948 (Δ −3.8 ppm).

4.3.2.3. (E)-Pent-2-en-4-ynoic acid [4-(3-chloro-4-fluorophenylamino)-3-cyano-7-ethoxyquinolin-6-yl]-amide (10). Yellow solid, 20% yield, R_f = 0.13 (Et_2O); ^{1}H NMR (500 MHz, $CDCl_3$) δ 9.10 (s, 1H), 8.56 (s, 1H), 8.09 (s, 1H), 7.39 (s, 1H), 7.35 (br s, 1H), 7.24 (dd, J = 6.3, 2.7, 1H), 7.16 (t, J = 8.6, 1H), 7.08 (ddd, J = 2.8, 3.9, 8.7, 1H), 6.82 (dd, J = 1.6, 15.4, 1H), 6.55 (d, J = 15.4, 1H), 4.33 (q, J = 7.0, 2H), 3.40 (dd, J = 0.4, 2.4, 1H), 1.58 (t, J = 7.0, 3H); ^{13}C NMR (126 MHz, $CDCl_3$) δ 162.6 (s), 156.6 [s (d, J_{CF} = 249.0)], 152.2 (d), 151.3 (s), 150.0 (s), 147.6 (s), 135.6 (s), 134.2 (d), 128.1 (s), 126.9 (d), 124.6 [d (d, J_{CF} = 7.1)], 122.9 (d), 121.9 [s (d, J_{CF} = 19.1)], 117.2 [d (d, J_{CF} = 22.3)], 116.5 (s), 113.2 (s), 109.9 (d), 108.8 (d), 89.2 (s), 86.3 (d), 80.3 (s), 65.3 (t), 14.5 (q); ^{19}F NMR (376 MHz, CDCl3) δ −117.0; IR: ν_{max} 3300, 2925, 2361, 2342, 2214, 1670, 1624, 1539, 1498, 1458, cm^{-1}; MS (ESI): m/z (%) 435 [MH^+] (100); HR-MS (ESI) calcd for $C_{23}H_{17}N_4O_2FCl$: 435.1024, found 435.1018 (Δ −1.4 ppm).

4.3.2.4. {(E)-3-[4-(3-Chloro-4-fluorophenylamino)-3-cyano-7-(2-fluoroethoxy)-quinolin-6-ylcarbamoyl]-allyl}-methylcarbamic acid tert-butyl ester (Boc-20). Yellow oil, 61% yield; R_f = 0.38 (AcOEt); ^{1}H NMR (500 MHz, $CDCl_3$) δ 9.15 (s, 1H), 8.57 (s, 1H), 8.10 (s, 1H), 7.40 (br s, 2H), 7.31–7.25 (m, 1H), 7.21–7.14 (m, 1H), 7.14–7.07 (m, 1H), 6.93 (dt, J = 5.0, 15.2, 1H), 6.13–5.98 (m, 1H), 4.90 (dm, J = 47.9, 2H), 4.50 (dm, J = 27.3, 2H), 4.06 (br s, 2H), 2.91 (br s, 3H), 1.48 (s, 9H); ^{13}C NMR (126 MHz, $CDCl_3$) δ 163.6 (s), 156.6 [s (d, J_{CF} = 284.1)], 155.8 (s), 152.3 (d), 150.6 (s), 150.0 (s), 147.1 (s), 142.6 and 142.2 (d), 135.5 (s), 128.4 (s), 126.9 (d), 124.6 (d), 123.5 (d), 121.8 [s (d, J_{CF} = 19.6)], 117.2 [d (d, J_{CF} = 22.3)], 116.5 (s), 113.8 (s), 110.0 (d), 109.2 (d), 100.0 (s), 85.4 [t (d, J_{CF} = 174.1)], 80.9 (s), 68.4 [t (d, J_{CF} = 19.5)], 50.0 and 49.4 (t), 34.6 and 34.5 (q), 29.7 (s, 3C); MS (ESI): m/z (%); 572 [MH^+] (100); HR-MS (ESI) calcd for $C_{28}H_{29}N_5O_4ClF_2$: 572.1876, found 572.1868 (Δ −1.4 ppm).

4.3.3. General procedure for the synthesis of compounds 6, 16, 20 and 21

Quinoline **5**, **8**, **Boc-16** or **Boc-20** (1 equiv) were dissolved in 1,4-dioxane (0.03 M) and concd HCl (0.003 M) was added dropwise at rt. The mixture was stirred 30 min—1 h and the precipitate was collected and washed with dioxane and Et_2O and dried in vacuo to give the title compounds as HCl salts.

4.3.3.1. (E)-4-(Methylamino)-but-2-enoic acid [4-(3-chloro-4-fluorophenylamino)-3-cyano-7-ethoxyquinoline-6-yl] amide hydrochloride (6·HCl). Yellow solid; 78% yield; ^{1}H NMR (400 MHz, MeOD): δ 9.24 (s, 1H), 8.87 (s, 1H), 7.72 (dd, J = 6.5, 2.5 Hz, 1H), 7.52 (ddd, J = 6.5, 8.7, 2.5, 1H), 7.48–7.36 (m, 2H), 7.00 (dt, J = 15.2, 1H), 6.82 (dt, J = 15.2, 1.4, 1H), 4.47 (q, J = 7.0, 2H), 3.92 (d, J = 6.4, 2H), 2.78 (s, 3H), 1.62 (t, J = 7.0, 3H); ^{13}C NMR (101 MHz, MeOD): δ 163.5 (s), 158.1 [s (d, J_{CF} = 250.1)], 155.7 (s), 154.5 (s), 147.5 (d), 146.1 (s), 136.6 (s), 134.6 (d), 133.8 (s), 129.6 (d), 129.4 (d), 127.7 [d (d, J_{CF} = 7.8 Hz)], 121.3 [s (d, J_{CF} = 19.2)], 117.0 [d (d, J_{CF} = 22.7 Hz)], 114.0 (d), 113.1 (s), 111.9 (s), 100.3 (d), 86.7 (s), 66.8 (t), 48.9 (t), 32.2 (q), 13.2 (q); IR (solid): ν_{max} 3377, 2938, 2687, 2225, 1634, 1530, 1491, 1258, 1060, 880 cm^{-1}; MS (ESI): m/z (%) 454 [MH$^+$] (48), 248 (100); HR-MS (ESI) calcd for $C_{23}H_{22}ClFN_5O_2$: 454.1446, found 454.1459 (Δ 2.9 ppm).

4.3.3.2. (E)-4-{[1-(2-Fluoroethyl)-1H-[1,2,3]triazol-4-ylmethyl]-amino}-but-2-enoic acid [4-(3-chloro-4-fluoro-phenylamino)-3-cyano-7-ethoxy-quinolin-6-yl]-amide hydrochloride (16). Yellow solid; 99% yield; ^{1}H NMR (500 MHz, DMSO-d_6) δ 10.99 (br s, 1H), 9.93 (s, 1H), 9.83 (s, 1H), 9.12 (br s, 1H), 8.97 (s, 1H), 8.33 (s, 1H), 7.72 (d, J = 6.1, 1H), 7.61 (s, 1H), 7.53 (t, J = 9.0, 1H), 7.47–7.41 (m, 1H), 6.87 (dt, J = 15.5, 6.35, 1H), 6.78 (d, J = 15.6, 1H), 4.84 (dm, J = 32.3, 2H), 4.79–4.74 (m, 2H), 4.34 (q, J = 7.0, 2H), 4.29 (t, J = 4.9, 2H), 3.86 (br dd, J = 11.6, 5.9, 2H), 1.49 (t, J = 7.0, 3H).; ^{19}F NMR (376 MHz, DMSO-d_6) δ −117.9, −222.0; ^{13}C NMR (101 MHz, DMSO-d_6) δ 162.7 (s), 155.3 [s (d, J_{CF} = 422.7)] 155.1 (s), 154.9 (s), 149.3 (d), 138.5 (s), 135.6 (s), 134.6 (d), 129.4 (d), 128.6 (s), 128.4 (s), 127.8 [d (d, J_{CF} = 7.5)], 126.6 (d), 126.0 (d), 119.8 [s (d, J_{CF} = 18.9)], 117.3 [d (d, J_{CF} = 22.3)], 116.4 (d), 114.8 (s), 112.5 (s), 102.9 (d), 86.9 (s), 81.9 [t, (d, J_{CF} = 168.3)], 65.3 (t), 50.2 [t, (d, J_{CF} = 19.4)], 46.6 (t), 40.8 (t), 14.1 (q); IR (solid): ν_{max} 3371, 2937, 2732, 1635, 1533, 1493, 1260, 1020, 823 cm^{-1}; MS (ESI): m/z (%) 567 [MH$^+$] (80), 440 (100); HR-MS (ESI) calcd for $C_{27}H_{26}N_8O_2F_2Cl$: 567.1835, found 567.1841 (Δ 1.1 ppm).

4.3.3.3. (E)-4-Methylamino-but-2-enoic acid [4-(3-chloro-4-fluorophenylamino)-3-cyano-7-(2-fluoroethoxy)-quinolin-6-yl]-amide hydrochloride (20). Yellow solid; 67% yield; ^{1}H NMR (400 MHz, MeOD) δ 9.27 (s, 1H), 8.93 (br s, 1H), 7.73 (dd, J = 6.5, 2.5, 1H), 7.55–7.48 (m, 2H), 7.48–7.40 (m, 1H), 7.01 (dt, J = 15.1, 6.5, 1H), 6.83 (d, J = 15.4, 1H), 5.06–4.87 (dm, 2H), 4.67 (dm, J = 28.7, 2H), 3.93 (d, J = 6.5, 2H), 2.79 (s, 3H); ^{19}F NMR (376 MHz, MeOD) δ −118.1, −223.9; ^{13}C NMR (101 MHz, MeOD) δ 164.8 (s), 159.7 [s (d, J_{CF} = 255.2)], 156.9 (s), 156.2 (s), 149.55 (d), 138.6 (s), 135.5 (d), 135.3 (s), 131.2 (d), 131.0 (s), 130.8 (d), 128.9 [d (d, J_{CF} = 7.9)], 122.9 [s (d, J_{CF} = 19.3)], 118.6 [d (d, J_{CF} = 22.8)], 116.2 (d), 114.4 (s), 113.8 (s), 102.5 (d), 101.9 (s), 82.7 [t (d, J_{CF} = 169.7)], 71.0 [t, (d, J_{CF} = 19.8)], 50.2 (t), 33.3 (q); IR (solid): ν_{max} 3395, 2926, 2224, 1532, 1494, 1259, 1059, 835 cm^{-1}; MS (ESI): m/z (%); 472 [MH$^+$] (52), 257 (100); HR-MS (ESI) calcd for $C_{23}H_{21}N_5O_2ClF_2$: 472.1354, found 472.1342 (Δ −2.1 ppm).

4.3.3.4. (E)-4-Prop-2-ynylaminobut-2-enoic acid [4-(3-chloro-4-fluorophenylamino)-3-cyano-7-ethoxyquinolin-6-yl]-amide hydrochloride (21). Yellow solid; 99% yield; ^{1}H NMR (400 MHz, DMSO-d_6) δ 11.02 (br s, 1H), 9.98 (s, 1H), 9.83 (s, 2H), 9.14 (s, 1H), 8.98 (s, 1H), 7.75 (d, J = 6.6, 1H), 7.61–7.57 (m, 1H), 7.55 (t, J = 8.5, 1H), 7.50–7.44 (m, 1H), 6.90–6.78 (m, 1H), 6.81 (t, J = 11.9, 1H), 4.36 (q, J = 7.0, 2H), 3.95 (s, 2H), 3.87 (d, J = 5.4, 2H), 3.76 (t, J = 2.3, 1H), 1.50 (t, J = 6.9, 3H); ^{13}C NMR (101 MHz, DMSO-d_6) δ 162.8 (s), 156.3 [s (d, J_{CF} = 247.0)], 155.2 (s), 153.2 (s), 149.3 (d), 139.6 (s), 135.4 (s), 134.3 (d), 129.6 (d), 128.6 (d), 127.9 (s), 126.7 [d (d, J_{CF} = 7.0)], 119.9 [s (d, J_{CF} = 18.9)], 117.4 [d (d, J_{CF} = 22.3)], 116.3 (d), 114.7 (s), 112.5 (s), 102.9 (d), 86.9 (s), 79.8 (d), 74.8 (s), 65.4 (t), 46.2 (t), 35.3 (t), 14.1 (q); IR (solid): ν_{max} 3404, 3291, 2932, 2601, 2424, 2223, 1687, 1578, 1489, 1452, 1258, 1032, 883 cm^{-1}; MS (ESI): m/z (%) 478 [MH$^+$] (100); HR-MS (ESI) calcd for $C_{25}H_{22}N_5O_2FCl$: 478.1446, found 478.1448 (Δ 0.4 ppm).

4.3.3.5. (E)-4-(Methylamino)-but-2-enoic acid [4-(3-chloro-4-fluorophenylamino)-3-cyano-7-ethoxy-quinoline-6-yl] amide (6). The quinoline hydrochloride **6·HCl** (39.0 mg, 0.08 mmol) was dissolved in water (1 mL) and K_2CO_3 (55 mg, 0.4 mmol) was added. The mixture was stirred 14 h at rt and the pale yellow precipitate was collected, washed with water and dried in vacuo to give the title compound **6** (27.1 mg, 78%) as a yellow solid.

^{1}H NMR (400 MHz, MeOD): δ 8.96 (s, 1H), 8.48 (s, 1H), 7.48–7.41 (m, 1H), 7.41–7.35 (m, 1H), 7.35–7.24 (m, 2H), 7.04 (dt, J = 15.4, 5.8 Hz, 1H), 6.50 (dt, J = 15.5, 1.5 Hz, 1H), 4.37 (q, J = 6.8 Hz, 2H), 3.44 (dd, J = 5.7, 1.0 Hz, 2H), 2.45 (s, 3H), 1.59 (t, J = 6.9 Hz, 3H).

4.3.3.6. (E)-4-[(2-Fluoroethyl) methyl amino]-but-2-enoic acid [4-(3-chloro-4-fluorophenylamino)-3-cyano-7-ethoxyquinoline-6-yl] amide (12). Quinoline **6** (32 mg, 0.07 mmol) was dissolved in dry CH_2Cl_2 (0.7 mL) and 1-fluoro-2-mesyloxy ethane (**11**, 13 mg, 0.09 mmol) and Et_3N (20 μL, 0.14 mmol) were added in turn. The mixture was stirred overnight, concentrated and directly purified by preparative silica TLC on silica gel (CH_2Cl_2/MeOH, 20:1; R_f = 0.28) to give quinoline **12** (11.5 mg, 33%) as a yellow solid.

^{1}H NMR (400 MHz, $CDCl_3$): δ 9.17 (s, 1H), 8.54 (s, 1H), 8.11 (s, 1H), 7.53 (s, 1H), 7.33 (s, 1H), 7.21 (dd, J = 6.3, 2.6, 1H), 7.12 (t, J = 8.6, 1H), 7.08–6.99 (m, 2H), 6.27 (dt, J = 15.2, 1.6, 1H), 4.59 (dt, J = 47.6, 4.8, 2H), 4.32 (q, J = 7.0, 2H), 3.33 (dd, J = 5.6, 3.1, 2H), 2.77 (dt, J = 28.0, 4.8, 2H), 2.39 (s, 3H), 1.60 (t, J = 7.0, 3H); ^{19}F NMR (376 MHz, $CDCl_3$): δ −117.5, −219.4; ^{13}C NMR (126 MHz, $CDCl_3$): δ 164.0 (s), 156.4 [s (d, J_{CF} = 248.7 Hz)], 152.2 (d), 151.2 (s), 149.9 (s), 147.4 (s), 143.9 (d), 135.7 (s), 128.3 (s), 126.7 (d), 125.3 (d), 124.3 [d (d, J_{CF} = 7.3 Hz)], 121.7 [s J_{CF} = 19.0)], 117.1 (s), 116.8 [d (d, J_{CF} = 24.8 Hz)], 113.3 (s), 109.4 (d), 108.8 (d), 88.9 (s), 82.1 [t, (d, J_{CF} = 168.0 Hz)], 65.2 (t), 58.6 (t), 57.0 [t, (d, J_{CF} = 19.7 Hz)], 42.9 (q), 14.5 (q); IR: ν_{max} 3250, 2924, 2212, 1685, 1622, 1537, 1498, 1458, 1393, 1215 cm^{-1}; MS (ESI): m/z (%) 500 [MH$^+$] (76), 271 (100); HR-MS (ESI) calcd for $C_{25}H_{25}N_5O_2F_2Cl$: 500.1665, found 500.1662 (Δ −0.6 ppm).

4.3.3.7. (E)-4-[(4-Fluorobenzyl) methylamino]-but-2-enoic acid [4-(3-chloro-4-fluorophenylamino)-3-cyano-7-ethoxyquinoline-6-yl] amide (13). Quinoline **6** (50 mg, 0.10 mmol) was suspended in dichloroethane (0.3 mL) and *p*-fluorobenzaldehyde (12 μL, 0.11 mmol) and acetic acid (10 μL) were added dropwise at rt. After 30 min, $NaBH(OAc)_3$ (32 mg, 0.15 mmol) was added and the mixture was stirred 14 h at rt. The mixture was quenched with a saturated solution of $NaHCO_3$ (1 mL) and extracted with CH_2Cl_2 (3 × 2 mL). The combined organic layers were dried over $MgSO_4$. After purification by plate silica TLC (CH_2Cl_2/MeOH, 20:1; R_f = 0.37), the title compound **13** was obtained (12 mg, 21%) as a yellow solid.

^{1}H NMR (400 MHz, $CDCl_3$): δ 9.18 (s, 1H), 8.52 (s, 1H), 8.07 (s, 1H), 7.66 (s, 1H), 7.34–7.27 (m, 4H), 7.12 (dd, J = 6.3, 2.5, 1H), 7.12–7.00 (m, 4H), 6.96 (dt, J = 8.3, 3.4, 1H), 6.24 (dt, J = 15.3, 1.6, 1H), 4.32 (q, J = 7.0, 2H), 3.53 (s, 2H), 3.23 (dd, J = 5.7, 1.0, 2H), 2.25 (s, 3H), 1.61 (t, J = 6.7, 3H); ^{19}F NMR (376 MHz, $CDCl_3$): δ −117.6, −115.5; ^{13}C NMR (126 MHz, $CDCl_3$): δ 163.9 (s), 162.1 [s J_{CF} = 245.1 Hz], 156.5 [s (d, J_{CF} = 249.2 Hz)], 152.1 (d), 151.2 (s), 149.8 (s), 147.5 (s), 144.5 (d), 135.7 (s), 134.2 (s), 130.3 [d (d, J_{CF} = 7.8 Hz, 2C)], 128.5 (s), 126.8 (d), 125.2 (d), 124.3 [d (d, J_{CF} = 7.4 Hz)], 121.6 [s (d, J_{CF} = 21.0)], 117.2 (s), 116.9 [d (d, J_{CF} = 43.3 Hz)], 115.2 [d (d, J_{CF} = 21.4 Hz, 2C)], 113.3 (s),

109.3 (d), 108.8 (d), 89.1 (s), 65.2 (t), 61.3 (t), 57.8 (t), 42.5 (q), 14.6 (q); IR: ν_{max} 3380, 2922, 2220, 1680, 1620, 1537, 1458 cm^{-1}; MS (ESI): *m*/*z* (%) 562 [MH^+] (50), 454 (100); HR-MS (ESI) calcd for $C_{30}H_{27}N_5O_2F_2Cl$: 562.1821, found 562.1828 (1.2 ppm).

4.3.4. General procedure for the synthesis of compounds 15 and Boc-16

Quinoline **8** or **10** (1 equiv) was dispersed in water (0.15 M) and fluoro ethylazide **14** (0.5 M solution in DMF, 2 equiv), $CuSO_4$ (0.3 equiv) and Cu powder (0.3 equiv) were added. The mixture was heated by microwave irradiation at 125 °C for 15 min and diluted with water and AcOEt. The phases were separated and the aqueous phase was extracted with AcOEt. The combined organic layers were dried over $MgSO_4$. The crude residue was purified by FC to give the compounds **Boc-16** or **15**, respectively.

4.3.4.1. (E)-N-[4-(3-Chloro-4-fluorophenylamino)-3-cyano-7-ethoxyquinolin-6-yl]-3-[1-(2-fluoroethyl)-1H-[1,2,3]triazol-4-yl]-acrylamide (15). Yellow solid; 32% yield; R_f = 0.28 (AcOEt/MeOH, 1:1); ^{1}H NMR (500 MHz, $CDCl_3$) δ 9.20 (s, 1H), 8.55 (br s, 1H), 8.26 (s, 1H), 7.83 (s, 1H), 7.68 (d, *J* = 15.3, 1H), 7.52 (br s, 1H), 7.48 (s, 1H), 7.29 (dd, *J* = 6.2, 2.6, 1H), 7.18 (t, *J* = 8.6, 1H), 7.15–7.09 (m, 1H), 7.05 (d, *J* = 15.3, 1H), 4.84 (dm, *J* = 46.7, 2H), 4.73 (dm, *J* = 27.1, 2H), 4.35 (q, *J* = 7.0, 2H), 1.61 (t, *J* = 7.0, 3H); ^{19}F NMR (376 MHz, $CDCl_3$) δ −116.1, −220.7; ^{13}C NMR (126 MHz, $CDCl_3$) δ 163.89 (s), 156.73 [s (d J_{CF} = 250.1)], 151.62 (d), 151.38 (s), 150.29 (s), 148.88 (s), 143.57 (s), 135.41 (s), 130.30 (d), 128.75 (s), 127.08 (d), 124.92 (d), 124.72 [d (d, J_{CF} = 6.4)], 122.24 (d), 121.91 [s (d, J_{CF} = 18.9)], 117.23 [d (d, J_{CF} = 22.4)], 116.29 (s), 113.17 (s), 109.54 (d), 108.05 (d), 99.96 (s), 81.36 [t (d, J_{CF} = 173.0)], 65.49 (t), 50.73 [t (d, J_{CF} = 20.5)], 14.61 (q); IR: ν_{max} 3266, 2954, 2212, 1623, 1538, 1498, 1460, 1224, 1036 cm^{-1}; MS (ESI): *m*/*z* (%) 524 [MH^+] (100); HR-MS (ESI) calcd for $C_{25}H_{21}N_7O_2F_2Cl$: 524.1413, found 524.1404 (Δ −1.7 ppm).

4.3.4.2. {(E)-3-[4-(3-Chloro-4-fluorophenylamino)-3-cyano-7-ethoxyquinolin-6-ylcarbamoyl]-allyl}-[1-(2-fluoroethyl)-1H-[1,2,3]triazol-4-ylmethyl]-carbamic acid tert-butyl ester (Boc-16). Yellow semisolid; 19% yield; R_f = 0.36 (eluent: AcOEt/MeOH, 10:1); ^{1}H NMR (400 MHz, $CDCl_3$) δ 9.15 (s, 1H), 8.58 (s, 1H), 8.14 (s, 1H), 7.73 (dd, *J* = 5.7, 3.3, 1H), 7.53–7.42 (m, 2H), 7.31 (dd, *J* = 6.2, 2.6, 1H), 7.21 (t, *J* = 8.5, 1H), 7.17–7.11 (m, 1H), 6.97–6.87 (m, 1H), 6.26–6.06 (m, 1H), 4.81 (dt, *J* = 46.8, 4.3, 2H), 4.69 (dm, *J* = 26.7, 2H), 4.58–4.50 (m, 2H), 4.42–4.34 (m, 2H), 4.22–4.13 (m, 2H), 1.63 (t, *J* = 6.8, 3H), 1.28 (s, 9H); ^{19}F NMR (376 MHz, $CDCl_3$) δ −59.9, −115.8; ^{13}C NMR (126 MHz, $CDCl_3$) δ 171.1 (s), 163.7 (s), 156.3 [s (d, J_{CF} = 249.0)], 152.1 (d), 151.3 (s), 149.9 (s), 147.3 (s), 145.2 and 144.9 (s), 142.2 and 141.8 (d), 135.6 (s), 128.2 (s), 126.7 (d), 124.4 (d), 124.3 [d (d, J_{CF} = 6.8)], 123.8 and 123.0 (d), 121.6 [s (d, J_{CF} = 19.1)], 117.0 [d (d, J_{CF} = 22.4)], 116.6 (s), 113.2 (s), 109.7 (d), 108.6 (d), 88.9 (s), 81.4 [t (d, J_{CF} = 162.1)], 80.8 (s), 65.2 (t), 50.5 [t (d, J_{CF} = 20.4)], 47.9 and 47.5 (t), 42.0 and 41.5 (t), 28.3 (q, 3C), 14.5 (q); IR: ν_{max} 2925, 2854, 2220, 1688, 1537, 1459, 1163 cm^{-1}; MS (ESI): *m*/*z* (%) 689 [MNa^+] (100), 667 [M^+]; HR-MS (ESI) calcd for $C_{32}H_{34}N_8O_4F_2Cl$: 667.2360, found 667.2354 (Δ −0.9 ppm).

4.3.4.3. N-[4-(3-Chloro-4-fluorophenylamino)-3-cyano-7-hydroxyquinolin-6-yl]-acetamide (18). The quinoline **17** (500 mg, 1.15 mmol) was suspended in dry CH_2Cl_2 (50 mL) and BBr_3 (1.0 M in CH_2Cl_2, 5.7 mL, 5.7 mmol) was added dropwise at rt. The mixture was stirred 14 h and quenched with water (20 mL). The yellow precipitate was collected, washed with water (50 mL), and dried in vacuo. The title compound **18** was obtained as a yellow solid (166 mg, 40%) and used in the next step without further purification.

^{1}H NMR (400 MHz, MeOD) δ 9.12 (s, 1H), 8.79 (s, 1H), 7.68 (dd, *J* = 1.5, 6.1, 1H), 7.51–7.45 (m, 1H), 7.41 (t, *J* = 8.7, 1H), 7.35 (s, 1H), 2.28 (s, 3H); ^{13}C NMR (101 MHz, MeOD) δ 170.9 (s), 158.2 [s (d, J_{CF} = 250.0)], 155.6 (s), 154.7 (s), 147.3 (d), 136.4 (s), 134.0 (s), 130.0 (s), 129.4 (d), 127.6 [d (d, J_{CF} = 7.9)], 121.4 [s (d, J_{CF} = 19.0)], 117.6 [d (d, J_{CF} = 22.8)], 113.7 (d), 113.1 (s), 111.4 (s), 102.3 (d), 86.1 (s), 22.7 (q); IR: ν_{max} 3357, 3018, 2925, 2228, 1613, 1539, 1495, 1469, 1238 cm^{-1}; MS (ESI): *m*/*z* (%) 371 [MH^+] (100), 144 (25); HR-MS (ESI) calcd for $C_{18}H_{13}N_4O_2ClF$: 371.0711, found 371.0707 (Δ −1.1 ppm).

4.3.4.4. 6-Amino-4-(3-chloro-4-fluorophenylamino)-7-(2-fluoroethoxy)-quinoline-3-carbonitrile (19). The quinoline **18** (25 mg, 0.06 mmol) was heated with K_2CO_3 (41.4 mg, 0.30 mmol) and 2-mesyloxy-1-fluoroethane (17 mg, 0.12 mmol) in DMF (1 mL) at 70 °C overnight. The mixture was cooled at rt, water (1 mL) was added and yellow solid was collected, washed with water (3 mL) and Et_2O (3 mL) and dried in vacuo. The yellow solid was then refluxed in water (0.5 mL) and concd HCl (0.5 mL) for 2.5 h then cooled at rt. The crude mixture was concentrated under reduced pressure, dissolved in water (2 mL) and neutralized with K_2CO_3. Quinoline **19** (8 mg, 53%) was collected as a yellow solid.

^{1}H NMR (400 MHz, MeOD) δ 8.30 (s, 1H), 8.25 (s, 1H), 7.33 (dd, *J* = 2.6, 6.4, 1H), 7.26 (s, 1H), 7.24–7.21 (m, 1H), 7.18–7.15 (m, 1H), 4.87 (dm, *J* = 47.7, 2H), 4.46 (dm, *J* = 28.6, 2H); ^{19}F NMR (376 MHz, MeOD) δ −122.4, −225.1; ^{13}C NMR (101 MHz, MeOD) δ 157.1 [s (d, *J* = 249.0)], 155.8 (s), 153.3 (s), 149.5 (d), 145.0 (s), 140.8 (s), 138.3 (s), 126.9 [d (d, *J* = 7.0)], 125.0 [d (d, J_{CF} = 7.3)], 122.2 [s (d, J_{CF} = 19.0)], 118.0 [d (d J_{CF} = 22.3)], 117.1 (s), 113.2 (d), 108.1 (s), 103.5 (s), 102.7 (d), 82.8 [t, (d J_{CF} = 169.2)], 69.4 [t, (d J_{CF} = 20.0)]; IR (solid): ν_{max} 3348, 2926, 2210, 1619, 1568, 1454, 1214, 1047, 869 cm^{-1}; MS (ESI): *m*/*z* (%) 375 [MH^+] (85), 355 (100); HR-MS (ESI) calcd for $C_{18}H_{14}N_4OClF_2$: 375.0824, found 375.0830 (Δ 1.6 ppm).

4.4. Radiochemistry

Under an atmosphere of nitrogen, a buffered solution (sodium phosphate buffer, pH 6.0, 250 mM) of sodium ascorbate (50 μL, 8.7 mg, 43.2 μmol) was added to a Wheaton vial (3 mL) containing an aqueous solution of copper(II) sulfate (50 μL, 1.7 mg pentahydrate, 7.0 μmol). After 1 min, a solution of alkyne **21** (2.1 mg, 4.4 μmol) in MeCN/water, 1:1 (50 μL) was added followed by distilled 2-[^{18}F]fluoroethylazide (94–740 MBq) in acetonitrile (100 μL). The mixture was heated at 80 °C for 15 min, the HPLC mobile phase [21% MeCN (0.085% H_3PO_4), 500 μL] was added and the resulting mixture was purified by preparative radio-HPLC. The isolated HPLC fraction was diluted with water (5 mL) and loaded onto a SepPak C18-light cartridge (Waters) that had been conditioned with ethanol (5 mL) and water (10 mL). The cartridge was subsequently flushed with water (5 mL) and [^{18}F]**16** eluted with ethanol (0.1 mL fractions). The product fraction was diluted with PBS to provide an ethanol content of 10–20% (v/v).

4.5. EGFR tyrosine kinase enzyme inhibition assay

The inhibitory activity of quinolines **1**, **6**, **12**, **13**, **15**, **16**, **20**, and **21** against EGFR kinase activity was measured by a time resolved fluorescence assay (DELFIA, Perkin–Elmer Life Sciences, Boston, MA, USA). The compounds were dissolved in DMSO and diluted in DMSO to give final concentrations of 0.0001–100,000 μg/mL. EGFR protein (E-3641, Sigma) was incubated with the compounds in a kinase buffer for 15 min at rt in accordance with manufacturer's instructions (DELFIA Tyrosine kinase kit; Perkin–Elmer). After 15 min at rt the kinase reaction was initiated by addition of 25 μM ATP, 25 mM $MgCl_2$, and 0.25 μM/L of biotinylated poly(Glu,

Ala, Tyr) in 10 mM HEPES buffer, pH 7.4. The reaction proceeded at rt for 1 h and was stopped by addition of 100 mM EDTA. The enzyme reaction solution was diluted and aliquots added to 96-well ELISA streptavidin plates with shaking for 1 h. The plates were washed and phosphorylated tyrosine was detected with Eu-labelled antiphosphotyrosine antibody (50 ng/well; PT66; Perkin–Elmer). After washing and enhancement steps, the plates were assessed in a Victor^3 multi-label counter (Perkin–Elmer) using the EGFR Europium protocol. The concentration of compound that inhibited 50% of receptor phosphorylation activity (IC_{50}) was estimated by non-linear regression analysis using GraphPad Prism (Version 4.0 for Windows, GraphPad Software, San Diego California USA).

4.6. Protein immunoblotting

The ability of the compounds to diffuse into cells and to inhibit EGFR was assessed by measuring inhibition of receptor phosphorylation by quinolines **1**, **6**, **12**, **13**, **15**, **16**, **20**, and **21** in A431 human epidermoid cancer cells (American Type Culture Collection, Manassas, VA, USA). The cells were maintained in DMEM (Sigma–Aldrich Company Ltd, Dorset, UK) supplemented with 10% fetal bovine serum (Lonza, UK), and 2 mM L-glutamine, 100 U/mL penicillin, 100 μg/mL streptomycin and 1 μg/mL fungizone (GIBCO) in six well plates incubated at 37 °C in a humidified incubator with 5% CO_2. The experiments were designed to assess irreversibility of EGFR inhibition by the compounds. Cells in exponential growth were incubated with quinolines **1**, **6**, **12**, **13**, **15**, **16**, **20**, and **21** at various concentrations for 3 h. EGF (100 ng/ml) was added to the cells during the last 15 min to induce p-EGFR. The medium was removed and replaced with fresh compound-free medium for 1 h. The last step was then repeated twice. The cells were then washed with cold PBS and lysed in RIPA buffer (Invitrogen Ltd, Paisley, UK) supplemented with protease and phosphatase inhibitor cocktails (Sigma–Aldrich Company Ltd, Dorset, UK). Lysates were clarified by centrifugation. The following antibodies were used: rabbit polyclonal antibody anti-p-EGFR (Cell signalling Technology, Denver, MA; 1:1000) and rabbit polyclonal antibody anti-EGFR (Santa Cruz Biotechnology, Santa Cruz, CA; 1:1000) and mouse monoclonal antibody anti-β-actin (Abcam, UK; 1:10000) as primary antibodies. The secondary antibodies were Goat anti-Rabbit IgG HRP (Santa Cruz Biotechnology Santa Cruz, CA; 1:2000) and Goat anti-Mouse IgG HRP (Autogen Bioclear, UK; 1:2000). The same procedure was used to assess EGFR and phospho-EGFR expression in HCT116 human colon carcinoma cells.

4.7. In vivo PET imaging and biodistribution

A431 and HCT116 xenografts were established by sc injection of 5×10^6 cells on the back of 6- to 8-week-old female *nu*/*nu* Balb/c mice (Harlan). All animal work was performed by licensed investigators in accordance with the United Kingdom's 'Guidance on the Operation of Animals (Scientific Procedures) Act 1986' (HMSO, London, United Kingdom, 1990).[42] When tumors reached ~100 mm^3, animals ($n = 3$) were scanned on a dedicated small animal CT/PET scanner (Siemens Multimodality Inveon, Siemens Molecular Imaging Inc., Knoxville, USA) following a bolus iv injection of 3.7 MBq of [^{18}F]**16**. Dynamic emission scans were acquired in list-mode format over 60 min. Cumulative images of the dynamic data (30–60 min) were iteratively reconstructed (OSEM3D) and used for visualization of radiotracer uptake to define the regions of interest (ROIs) with the Siemens Inveon Research Workplace software (three-dimensional ROIs were defined for each tumor). The count densities (counts/mL) were averaged for all ROIs at each of the 19 time points to obtain a time versus radioactivity curve (TAC). Tumor TACs were normalized to that total counts within the whole body at each of the time points to obtain the normalized uptake value expressed as %ID/mL. Direct [^{18}F]**16** tissue biodistribution was assessed subsequent to the PET scan. For this, mice were sacrificed by exsanguination via cardiac puncture under general anesthesia (isofluorane inhalation) and tissues were excised, weighted and immediately counted for fluorine-18 radioactivity on a Cobra-II Auto-Gamma counter (Packard Instruments, Meriden, CTA). Data were expressed as tissue to blood ratios and % injected dose per gram (%ID/g).

4.8. Metabolism studies

Non-tumor-bearing mice were injected intravenously with 3.7 MBq of radiotracer [^{18}F]**16**. Plasma and liver were collected at the indicated time and were snap-frozen in liquid nitrogen for subsequent HPLC analysis. For extraction, ice cold MeOH (1.5 mL) was added to plasma. The mixture was centrifuged (15,493*g*, 4 °C, 3 min) and the resulting supernatant was evaporated to dryness under vacuum at 40 °C using a rotary evaporator. Liver samples were homogenized with ice cold MeOH (1.5 mL) using an IKA Ultra-Turrax T-25 homogenizer prior to centrifugation. The supernatant was then decanted and evaporated to dryness. The samples were re-suspended in HPLC mobile phase (1.2 mL) and filtered through a Whatman PTFE syringe filter (0.2 μm). The samples (1 mL) were analyzed by radio-HPLC on an Agilent 1100 series HPLC system (Agilent Technologies, Stockport, UK) equipped with a γ-RAM model 3 gamma-detector (IN/US Systems Inc., Florida) and the Laura 3 software. The stationary phase comprised of a Waters μBondapak C18 reverse-phase column (300 mm × 7.8 mm) and the mobile phase comprised of water (0.085% H_3PO_4)/acetonitrile (0.085% H_3PO_4) (50:50) running in isocratic mode at a flowrate of 3 mL/min.

4.9. Extraction efficiency for plasma

To pre-weighed counting tubes ($n = 4$) Dulbecco's phosphate buffered saline (Sigma, Gillingham, UK) (200 μL) was added and to a further set of tubes ($n = 4$) mouse plasma extract (Mouse plasma lithium heparin—CD-1- Mixed Gender, pooled, Sera Laboratories International, West Sussex, UK) (200 μL) was added and the samples stored on ice until radiopharmaceutical addition. Formulated radiotracer [^{18}F]**16** was added to a set ($n = 4$) of blank counting tubes and to the tubes containing PBS or plasma. The samples were then incubated at 37 °C for 30 min and then snap-frozen using dry ice. Immediately prior to extraction samples were thawed on ice and ice cold methanol (1.5 mL) added. The samples were then centrifuged (15,493*g*, 4 °C, 3 min). The supernatant was then decanted and evaporated to dryness. The sample was then re-suspended in HPLC mobile phase (1.1 mL) and filtered (Whatman PTFE 0.2 μm, 13 mm filters). Total radioactivity for each sample (control: 100%, PBS extract: 95.4%, and plasma extract: 83.5%) was then measured on a Cobra-II Gamma Counter.

Acknowledgments

This work was funded by Cancer Research UK programme Grant C2536/A7602 and UK Medical Research Council core funding Grant U.1200.02.005.00001.01. We thank Rozanna Slade and Elizabeth Stevens for their contribution to the biology studies.

Supplementary data

Supplementary data (table of % injected dose per gram tissue of compound [^{18}F]**16** and chromatograms and chromatography purity of tested compounds) associated with this article can be found, in the online version, at doi:10.1016/j.bmc.2010.08.004.

References and notes

1. Marmor, M. D.; Skaria, K. B.; Yarden, Y. *Int. J. Radiat. Oncol. Biol. Phys.* **2004**, *58*, 903.
2. Bazley, L. A.; Gullick, W. J. *Endocr. Relat. Cancer* **2005**, *12*, S17.
3. Salomon, D. S.; Brandt, R.; Ciadiello, F.; Normanno, N. *Crit. Rev. Oncol. Hematol.* **1995**, *19*, 183.
4. Normanno, N.; Maiello, M. R.; de Luca, A. *J. Cell. Physiol.* **2002**, *194*, 13.
5. Woodburn, J. R. *Pharmacol. Ther.* **1999**, *82*, 241.
6. Huang, S.; Harari, P. M. *Proc. Am. Assoc. Cancer Res.* **1998**, 64.
7. Gridelli, C.; Maione, P.; Ferrara, M. L.; Rossi, A. *Oncologist* **2009**, *14*, 601.
8. Isamu, O. *FEBS J.* **2010**, *277*, 309.
9. Barker, A. J.; Gibson, K. H.; Grundy, W.; Godfrey, A. A.; Barlow, J. J.; Healy, M. P.; Woodburn, J. R.; Ashton, S. E.; Curry, B. J.; Scarlett, L.; Henthorn, L.; Richards, L. *Bioorg. Med. Chem. Lett.* **2001**, *11*, 1911.
10. Hidalgo, M.; Siu, L. L.; Nemunaitis, J.; Rizzo, J.; Hammond, L. A.; Takimoto, C.; Eckhardt, S. G.; Tolcher, A.; Britten, C. D.; Denis, L.; Ferrante, K.; Von Hoff, D. D.; Silberman, S.; Rowinsky, E. K. *J. Clin. Oncol.* **2001**, *19*, 3267.
11. Rabindran, S. K.; Discafani, C. M.; Rosfjord, E. C.; Baxter, M.; Floyd, M. B.; Golas, J.; Hallett, W. A.; Johnson, B. D.; Nilakantan, R.; Overbeek, E.; Reich, M. F.; Shen, R.; Shi, X.; Tsou, H.-R.; Wang, Y.-F.; Wissner, A. *Cancer Res.* **2004**, *64*, 3958.
12. Laheru, D.; Croghan, G.; Bukowski, R.; Rudek, M.; Messersmith, W.; Erlichman, C.; Pelley, R.; Jimeno, A.; Donehower, R.; Boni, J.; Abbas, R.; Martins, P.; Zacharchuk, C.; Hidalgo, M. *Clin. Cancer Res.* **2008**, *14*, 5602.
13. Mishani, E.; Abourbeh, G.; Eiblmaier, M.; Anderson, C. J. *Curr. Pharm. Des.* **2008**, *14*, 2983.
14. Ping Li, W.; Meyer, L. A.; Capretto, D. A.; Sherman, C. D.; Anderson, C. J. *Cancer Biother. Radiopharm.* **2008**, *23*, 158.
15. Eiblmaier, M.; Meyer, L. A.; Watson, M. A.; Fracasso, P. M.; Pike, L. J.; Anderson, C. J. *J. Nucl. Med.* **2008**, *49*, 1472.
16. Mulholland, G. K.; Zheng, Q.-H.; Winkle, W. L.; Carlson, K. A. *J. Nucl. Med.* **1997**, *38*, P141.
17. Seimbille, Y.; Phelps, M. E.; Czernin, J.; Silverman, D. H. S. *J. Labelled Compd. Radiopharm.* **2005**, *48*, 829.
18. Bonasera, T. A.; Ortu, G.; Rozen, Y.; Krais, R.; Freedman, N. M. T.; Chisin, R.; Gazit, A.; Levitzki, A.; Mishani, E. *Nucl. Med. Biol.* **2001**, *28*, 359.
19. VanBrocklin, V.; Lim, J. K.; Coffing, S. L.; Hom, D. L.; Negash, K.; Ono, M. Y.; Gilmore, J. L.; Bryant, I.; Riese, D. J. *J. Med. Chem.* **2005**, *48*, 7445.
20. Ortu, G.; Ben David, I.; Rozen, Y.; Freedman, N. M. T.; Chisin, R.; Levitzki, A.; Mishani, E. *Int. J. Cancer* **2002**, *101*, 360.
21. Mishani, E.; Abourbeh, G.; Rozen, Y.; Jacobson, O.; Laky, D.; Ben David, I.; Levitzki, A.; Shaul, M. *Nucl. Med. Biol.* **2004**, *31*, 469.
22. Abourbeh, G.; Dissoki, S.; Jacobson, O.; Litchi, A.; Daniel, R. B.; Laki, D.; Levitzki, A.; Mishani, E. *Nucl. Med. Biol.* **2007**, *34*, 55.
23. Dissoki, S.; Aviv, Y.; Laky, D.; Abourbeh, G.; Levitzki, A.; Mishani, E. *Appl. Radiat. Isot.* **2007**, *65*, 1140.
24. Dissoki, S.; Eshet, R.; Billauer, H.; Mishani, E. *J. Labelled Compd. Radiopharm.* **2009**, *52*, 41.
25. Kobus, D.; Giesen, Y.; Ullrich, R.; Backes, H.; Neumaier, B. *Appl. Radiat. Isot.* **2009**, *67*, 1977.
26. Yun, C.-H.; Mengwasser, K. E.; Toms, A. V.; Woo, M. S.; Greulich, H.; Wong, K.-K.; Meyerson, M.; Eck, M. J. *Proc. Natl. Acad. Sci. U.S.A.* **2008**, *105*, 2070.
27. Mishani, E.; Abourbeh, G.; Rozen, Y.; Jacobson, O.; Laky, D.; Ben David, I.; Levitzki, A.; Shaula, M. *Nucl. Med. Biol.* **2004**, *31*, 469.
28. Torrance, C. J.; Jackson, P. E.; Montgomery, E.; Kinzler, K. W.; Vogelstein, B.; Wissner, A.; Nunes, M.; Frost, P.; Discafani, C. M. *Nat. Med.* **2000**, *6*, 1024.
29. Wissner, A.; Overbeek, E.; Reich, M. F.; Floyd, M. B.; Johnson, B. D.; Mamuya, N.; Rosfjord, E. C.; Discafani, C.; Davis, R.; Shi, X.; Rabindran, S. K.; Gruber, B. C.; Ye, F.; Hallett, W. A.; Nilakantan, R.; Shen, R.; Wang, Y.-F.; Greenberger, L. M.; Tsou, H.-R. *J. Med. Chem.* **2003**, *46*, 49.
30. Smith, D. A.; Jones, B. C.; Walker, D. K. *Med. Res. Rev.* **1996**, *16*, 243.
31. Tsou, H.-R.; Overbeek-Klumpers, E. G.; Hallett, W. A.; Reich, M. F.; Floyd, M. B.; Johnson, B. D.; Michalak, R. S.; Nilakantan, R.; Discafani, C.; Golas, J.; Rabindran, S. K.; Shen, R.; Shi, X.; Wang, Y.-F.; Upeslacis, J.; Wissner, A. *J. Med. Chem.* **2005**, *48*, 1107.
32. Chew, W.; Rabindran, S. K.; Discafani-Marro, C.; McGinnis, J. P. I.; Wissner, A.; Wang, Y. WO2006127203, 2006.
33. Huisgen, R. *Angew. Chem., Int. Ed. Engl.* **1963**, *2*, 565.
34. Kolb, H. C.; Finn, M. G.; Sharpless, K. B. *Angew. Chem., Int. Ed.* **2001**, *40*, 2004.
35. Tornoe, C. W.; Christensen, C.; Meldal, M. *J. Org. Chem.* **2002**, *67*, 3057.
36. Hein, C.; Hein, C. D. *Pharm. Res.* **2008**, *25*, 2216.
37. Wei, X.; Taylor, R. J. K. *Tetrahedron Lett.* **1998**, *39*, 3815.
38. Glaser, M.; Årstad, E. *Bioconjugate Chem.* **2007**, *18*, 989.
39. Feldman, A. K.; Colasson, B.; Fokin, V. V. *Org. Lett.* **2004**, *6*, 3897.
40. Rewcastle, G. W.; Palmer, B. D.; Bridges, A. J.; Showalter, H. D. H.; Sun, L.; Nelson, J.; McMichael, A.; Kraker, A. J.; Fry, D. W.; Denny, W. A. *J. Med. Chem.* **1996**, *39*, 918.
41. Barnes, D. W. *J. Cell Biol.* **1982**, *93*, 1.
42. Workman, P.; Aboagye, E. O.; Balkwill, F.; Balmain, A.; Bruder, G.; Chaplin, D. J.; Double, J. A.; Everitt, J.; Farningham, D. A. H.; Glennie, M. J.; Kelland, L. R.; Robinson, V.; Stratford, I. J.; Tozer, G. M.; Watson, S.; Wedge, S. R.; Eccles, S. A. *Br. J. Cancer* **2010**, *102*, 1555.
43. Wissner, A.; Berger, D. M.; Boschelli, D. H.; Floyd, J.; Brawner, M.; Greenberger, L. M.; Gruber, B. C.; Johnson, B. D.; Mamuya, N.; Nilakantan, R.; Reich, M. F.; Shen, R.; Tsou, H.-R.; Upeslacis, E.; Wang, Y. F.; Wu, B.; Ye, F.; Zhang, N. *J. Med. Chem.* **2000**, *43*, 3244.
44. Block, D.; Coenen, H. H.; Stöcklin, G. *J. Labelled Compd. Radiopharm.* **1987**, *24*, 1029.
45. Haka, M. S.; Kilbourn, M. R.; Watkins, G. L.; Toorongian, S. A. *J. Labelled Compd. Radiopharm.* **1989**, *27*, 823.
46. Glaser, M.; Robins, E. G. *J. Labelled Compd. Radiopharm.* **2009**, *52*, 407.